

A single ion as a three-body reaction center in an ultracold atomic gas

Arne Härter,¹ Artjom Krüchow,¹ Andreas Brunner,¹ Wolfgang Schnitzler,¹ Stefan Schmid,¹ and Johannes Hecker Denschlag¹

¹*Institut für Quantenmaterie, Universität Ulm, 89069 Ulm, Germany*

(Dated: April 3, 2024)

We report on three-body recombination of a single trapped Rb^+ ion and two neutral Rb atoms in an ultracold atom cloud. We observe that the corresponding rate coefficient K_3 depends on collision energy and is about a factor of 1000 larger than for three colliding neutral Rb atoms. In the three-body recombination process large energies up to several 0.1 eV are released leading to an ejection of the ion from the atom cloud. It is sympathetically recooled back into the cloud via elastic binary collisions with cold atoms. Further, we find that the final ionic product of the three-body processes is again an atomic Rb^+ ion suggesting that the ion merely acts as a catalyzer, possibly in the formation of deeply bound Rb_2 molecules.

PACS numbers: 34.50.-s, 34.50.Lf, 37.10.-x, 37.10.Rs

Early on in the quest for ultracold quantum gases three-body recombination played a crucial role as a limiting factor for Bose-Einstein condensation. It was first investigated in spin-polarized hydrogen [1] and somewhat later for alkali atoms [2, 3]. For samples with large scattering lengths three-body processes can be resonantly modified through the formation of Efimov states [4]. Recently, three-body recombination was investigated with single atom resolution [5]. Combining ultracold atoms with cold trapped ions is an emerging field where large scattering cross sections naturally come into play due to the comparatively long range $1/r^4$ polarization interaction potential. Two-body collisions between atoms and ions in the low energy regime have been recently studied [6–12]. In this letter, we report on three-body collisions involving two ultracold ^{87}Rb atoms and a $^{87}\text{Rb}^+$ ion at mK temperatures.

The ion in our experiment can be regarded as a reaction center, facilitating molecule formation through its large interaction radius. For the work presented here, it is essential that we work with ions and atoms of the same species. This renders charge transfer reactions irrelevant, which otherwise would strongly constrain our measurements. Since no accessible optical transition is available for Rb^+ , it is not amenable to laser-cooling and cannot be imaged. We therefore detect the ion and investigate its dynamics in an indirect way, i.e. through its action on the atom cloud. In our experiments, we place a single ion into the center of an atomic sample resulting in a continuous loss of atoms due to elastic atom-ion collisions. This behavior is interrupted when a highly energetic three-body process ejects the ion from the atom cloud. By examining the statistics of ion-induced atom loss in hundreds of repetitions of the experiment, we can investigate a number of important details of the three-body process, such as its quadratic density-dependence, the energy that it releases, its rate coefficient K_3 and the dependence of K_3 on collisional energy. We also obtain information on the reaction products. As an important byproduct, our measurements also demonstrate sympathetic cooling of an ion from eV energies down to about 1 mK using an ultracold buffer gas.

The atom-ion collision experiments are conducted in a hybrid apparatus (for details see [13]) where a single $^{87}\text{Rb}^+$ ion, trapped in a linear Paul trap, is brought in contact with an ul-

tracold cloud of spin polarized ^{87}Rb atoms ($F = 1, m_F = -1$). The atom cloud is previously prepared at a separate location from where it is transported to the Paul trap and loaded into a far off-resonant crossed optical dipole trap. The dipole trap is at first spatially separated from the trapped ion by about $50 \mu\text{m}$. To start the atom-ion collision experiments it is then centered on the ion with μm precision within a few 100 ms. At this point the atom cloud consists of $N_{\text{at}} \approx 4.0 \times 10^4$ atoms at a temperature of $T_{\text{at}} \approx 1.2 \mu\text{K}$ and a peak density $n_{\text{at}} \approx 1.1 \times 10^{12} \text{cm}^{-3}$. At trapping frequencies of (190, 198, 55) Hz this results in a cigar shaped cloud with radial and axial extensions of about $10 \mu\text{m}$ and $35 \mu\text{m}$, respectively.

The single Rb^+ ion is confined in a Paul trap driven at a frequency of 4.17 MHz resulting in radial and axial trapping frequencies of 350 kHz and 72 kHz, respectively. As the trap is about 4 eV deep, the ion remains trapped on timescales of days and can typically be used for thousands of experimental cycles. It is initially produced by photoionization of an atom from a cold Rb cloud in the Paul trap [14]. Typical kinetic energies E_{ion} of the ion after sympathetic cooling in the atom cloud are about a few $\text{mK} \cdot k_B$ where k_B is the Boltzmann factor. This energy scale is mainly set by two quantities: (1) The excess micromotion (eMM) [15] in the Paul trap whose main part we can control by compensating stray electric fields [14]. (2) Heating effects induced by the interplay of micromotion and elastic collisions [16–18].

As described in [9], an ion immersed in an ultracold atom cloud leads to atom loss by expelling atoms from the shallow optical trap ($\approx 10 \mu\text{K} \cdot k_B$ trap depth) via elastic collisions. The radio frequency (rf) driven micromotion is a constant source of energy which drives these loss-afflicting collisions. Figure 1a shows such a decay of an atom cloud at relatively low densities ($\approx 10^{11} \text{cm}^{-3}$) and relatively high ion energies ($\approx 35 \text{mK} \cdot k_B$ [19]). Plotted is the number of remaining atoms after an atom-ion interaction time τ . Each data point corresponds to a single measurement. Overall, the plot shows a relatively smooth decay of the atom cloud with a relative scatter of the atom number of less than 10%. This changes drastically when we carry out the experiments at low ion energies ($\approx 0.5 \text{mK} \cdot k_B$ [19]) and larger densities ($\approx 10^{12} \text{cm}^{-3}$) (Fig. 1b). Here, the scatter dramatically increases with τ and

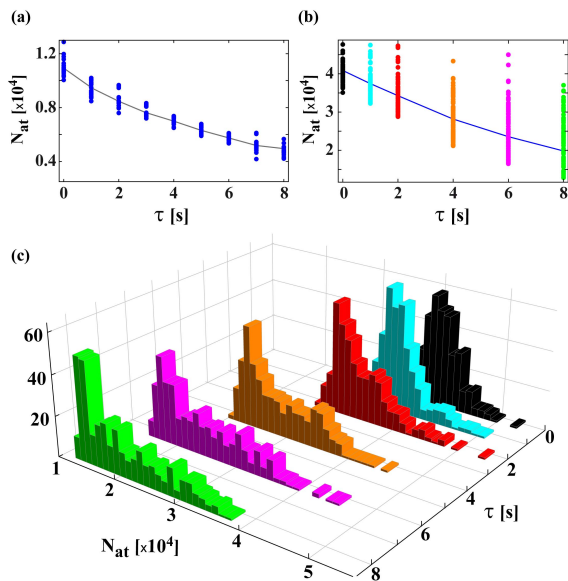


FIG. 1. Decay of the atom cloud under influence of a single trapped ion. (a) Remaining atom numbers after interaction time τ for an ion with $E_{\text{ion}} \approx 35 \text{ mK} \cdot k_B$ [19] and $n_{\text{at}} \approx 10^{11} \text{ cm}^{-3}$. The solid line indicates the decay of the mean atom number. (b) Same as (a) but $E_{\text{ion}} \approx 0.5 \text{ mK} \cdot k_B$ [19] and $n_{\text{at}} \approx 10^{12} \text{ cm}^{-3}$. (c) Histograms of the data shown in (b). The vertical axis counts the number of incidents for a particular atom number N_{at} and interaction time τ .

is on the order of the number of lost atoms. In Fig. 1c histograms of the data in Fig. 1b are shown. With increasing time τ the initial normal distribution becomes bimodal as a striking tail towards large atom numbers emerges. At the tips of the tails we find cases where even after interaction times of several seconds barely any atoms have been lost, a signature of missing atom-ion interaction. Apparently, sporadically the ion is ejected from the atom cloud and promoted onto a large orbit for a period of time during which atom-ion collisions are negligible (Fig. 2a). In principle, this is reminiscent of the energy distributions with high energy tails that have recently been predicted for trapped ions immersed in a buffer gas [16, 17]. However, it turns out that such an explanation is inconsistent with our observations [20]. Rather, we find that it is a three-body recombination process involving the ion and two neutrals that ejects the ion from the cloud. If, for example, a ground state molecule is formed, binding energies on the order of 0.5 eV can be released. Due to the large trap depth the ion is not lost in such an event, but it is recoiled back into the cloud through binary collisions after some time.

Figure 2b illustrates in a simple picture how the decay of the atom number over time can follow different paths. The solid trace T_1 shows the case when only binary atom-ion collisions occur. Such traces result in the narrow peak of the atom number distribution sketched on the right of Fig. 2b. Traces T_2 and T_3 exhibit three-body collisions at points E_2 and E_3 . At point R_2 the ion reenters the atom cloud after recoiling. Rare three-body events and long interruption times t_{out} result in a

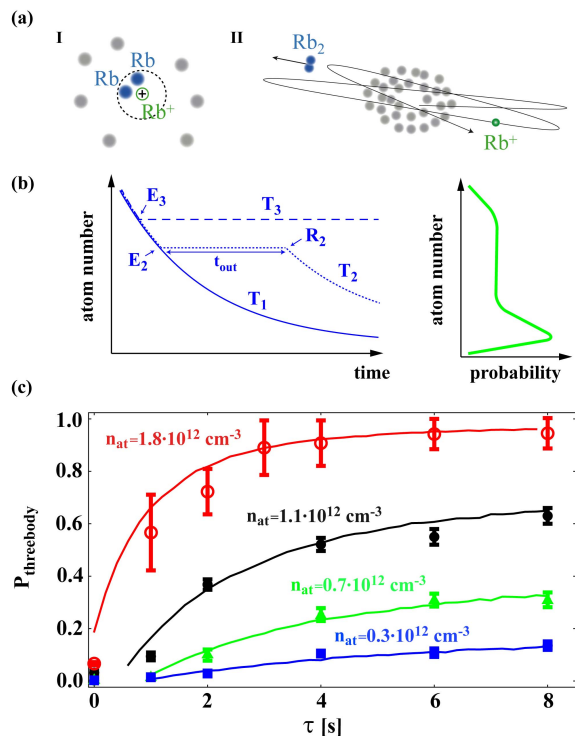


FIG. 2. (a) Illustration of an atom-atom-ion collision. (I) Two atoms simultaneously enter the interaction radius of the ion and a three-body process takes place. (II) The three-body reaction ejects the ion onto a trajectory much larger than the atom cloud. (b) Illustration of our simple model. *Left*: Various possible time traces for the atom number. If only binary atom-ion collision occur the atomic sample decays exponentially (Trace T_1). Three-body events (E_2 , E_3) interrupt the atom loss until the atom is recoiled and reenters the sample at point R_2 (Traces T_2 and T_3). *Right*: Sketch of the resulting atom number distribution when averaging over many experimental runs. (c) Plot of the probability $P_{\text{threebody}}$ for initial atomic densities $(1.8, 1.1, 0.7, 0.3) \times 10^{12} \text{ cm}^{-3}$ and atom numbers $(6.5, 4.0, 2.8, 1.6) \times 10^4$, respectively. The solid lines are results of the numerical simulation.

long tail of the distribution. We can reproduce the histograms in Fig. 1 with a simple Monte Carlo type simulation. We assume an initial normal distribution of the atom number which then decays exponentially with the binary atom-ion collision rate $K_2 n_{\text{at}}$. Here, $K_2 \approx 5 \times 10^{-9} \text{ cm}^3/\text{s}$ is a rate constant given by the product of the elastic cross section and the ion velocity. A three-body event, occurring at a rate $K_3 n_{\text{at}}^2$, interrupts this decay for a period t_{out} . As the ion can only be recoiled by the atomic sample, we assume the rate for reentry of the ion into the atom cloud to be proportional to the number of atoms $1/\langle t_{\text{out}} \rangle = N_{\text{at}}/c_{\text{out}}$ with c_{out} being a constant depending on the trap parameters. In order to fix the model parameters and rate constants it is convenient to carry out a data analysis as follows. We sum up the number of events in the tail of the distributions shown in Fig. 1 for each τ and divide by the total number of measurements to obtain the probability $P_{\text{threebody}}$ that at least one three-body process takes place within time

τ . These data are plotted as the filled black circles in Fig. 2c (data set with $n_{\text{at}} \approx 1.1 \times 10^{12} \text{ cm}^{-3}$). The corresponding errorbars mainly reflect the difficulty to unambiguously assign data points to the peak or the tail of the distribution where both parts of the bimodal distribution strongly overlap. Besides the data of Fig. 1c, Fig. 2c also contains data at three additional atomic densities. All four data sets have in common that the number of three-body events first rapidly increases and subsequently levels off. The leveling off is due to the fact that the probability for a three-body reaction is strongly density-dependent. Closer inspection of the data sets reveals a peculiar feature. In the beginning of the interaction ($\tau \lesssim 1 \text{ s}$) only very few three-body events are detected for the lower density samples. We explain this delay by an initial phase of sympathetic cooling of the Rb^+ ion which experiences significant heating during the preparation time of the atom cloud ($\sim 30 \text{ s}$). In fact, we observe ion heating specifically during evaporative cooling where the rf is ramped from 70 to 3 MHz. From numerical calculations we estimate that recoiling times of about 1 s in atom clouds with $n_{\text{at}} \approx 10^{12} \text{ cm}^{-3}$ correspond roughly to ion kinetic energies of a few $100 \text{ K} \cdot k_{\text{B}}$. According to the calculations the ion will typically undergo several thousand binary collisions with cold atoms until it is sympathetically recooled to $\text{mK} \cdot k_{\text{B}}$ energies. We are able to describe all four data sets in Fig. 2c consistently with our simple Monte Carlo model (continuous lines). From independent fits to each data set we obtain nearly identical rate coefficients in the range $K_3 = 3.1 - 3.5 \times 10^{-25} \text{ cm}^6/\text{s}$. For each fit the initial cool-down time is accounted for by adjusting the starting time of the simulation. We note that the value for our atom-atom-ion K_3 rate coefficient is more than three orders of magnitude larger than the three-body coefficient for three colliding neutral ^{87}Rb atoms [2].

In order to challenge our analysis we have attempted to model the events that send the ion into orbit as two-body processes. The corresponding linear density dependence of the event rate yields much less consistent fit results. The two-body rate coefficients would differ by more than a factor of 3 when comparing the analysis of the data set for the lowest and the highest density. As a cautionary note, we point out that three-body recombination processes to weakly-bound molecular states with binding energies $\lesssim 10 \text{ meV}$ are not detected in our experiments as the ion will not leave the atom cloud. Thus, the true three-body coefficient may even be significantly larger. From our analysis we also extract an approximate value for the interruption time coefficient $c_{\text{out}} \approx 1.7 \times 10^5 \text{ s}$. For the typical atom numbers used here this results in several seconds of negligible atom-ion interaction following each ejection of the ion.

In a further experiment, we quantify the kinetic energy ΔE_{ion} gained by the ion in a three-body event. The idea is to lower the depth of the ion trap such that an ion with an energy of a few 0.1 eV escapes while a cold ion remains trapped. The trap depth is reduced to one of 5 values U_{red} by lowering one of the endcap voltages of the Paul trap within 300 ms. The voltage is held at this value for 200 ms and ramped back up

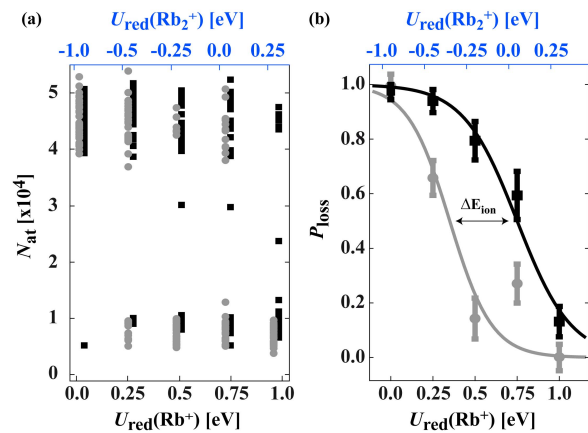


FIG. 3. Measuring the ion energy after a three-body process (black squares) and after purely binary collisions (grey dots). The trap depth is reduced to U_{red} . (a) If the ion “survives” this procedure in the trap it will subsequently induce atom loss in a freshly prepared cloud of atoms. Plotted is the remaining atom number. Data points with $N_{\text{at}} \lesssim 10^4$ signal the presence of an ion, while data points with $N_{\text{at}} \approx 4.5 \times 10^4$ correspond to a lost ion. For better visibility, we have slightly offset in energy the black squares from the grey dots. (b) Ion loss probability P_{loss} calculated from the data in (a). The continuous lines are guides to the eye.

within 200 ms. The trap depths U_{red} are indicated in Fig. 3. They have been computed using methods detailed in [21] for both Rb^+ (bottom abscissa scale) and Rb_2^+ (top). A negative trap depth value corresponds to non-trapping. After the trap depth reduction procedure is completed, the presence of the ion in the trap is probed via the loss it induces in a freshly prepared atom cloud containing about 5×10^4 atoms. For this probing procedure we deliberately apply an offset electric field of about 6 V/m to increase the eMM energy. In this way, we make three-body reactions unlikely and induce a rapid loss of atoms through binary atom-ion collisions. Figure 3a shows the remaining atom number after 6 s of interaction time. An atom number $\lesssim 1 \times 10^4$ indicates the presence of an ion while a number around 4.5×10^4 shows its absence. The clear splitting of the two groups of data allows for ion detection with an efficiency close to unity. In addition, this ion detection is energy resolved. Figure 3a contains two different plot symbols, distinguishing two classes of ions that have undergone a different prehistory before their energy resolved detection. Black plot symbols correspond to ions that have been promoted to a high energy orbit due to a three-body recombination. The recombination occurred during 4 s of atom-ion interaction and is detected through strongly reduced atom loss. Grey plot symbols correspond to ions where no suppression of atom loss was detected. These ions should in general have low kinetic energy. We now analyze the data points of Fig. 3a by calculating the probability for ion loss P_{loss} (see Fig. 3b). As expected, ions that were involved in a three-body recombination process can in general escape from deeper traps than cold ions. From the energy offset between the black and grey data we estimate

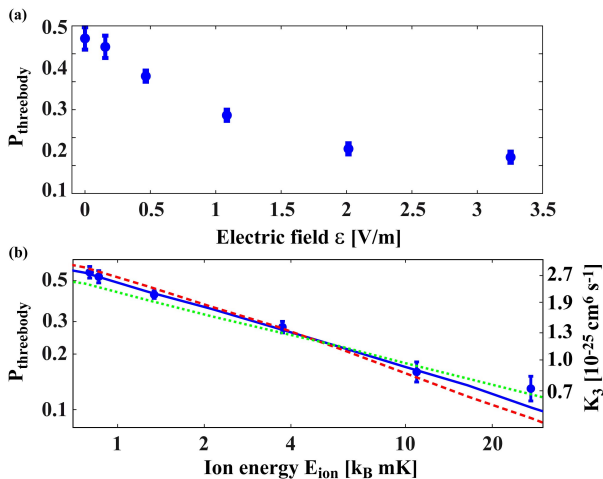


FIG. 4. (a): $P_{\text{threebody}}$ as a function of the external electric field. (b): Double-logarithmic plot of $P_{\text{threebody}}$ as a function of the ion energy E_{ion} [19]. A scale for the three-body coefficients K_3 as derived from the simulation is also given (see text for details).

the gained energy $\Delta E_{\text{ion}} \approx 0.4$ eV. We note that for trap depths $U_{\text{red}} \lesssim 0.25$ eV the probability of loss is high in general. This suggests that the stability of our trap is compromised at such shallow trapping potentials, limiting the accuracy with which we can determine the energy released in the three-body process. Still, we find a clear splitting between the black and grey data sets. Thus, a resolution of the measurement on the order of 0.1 eV seems plausible.

Mainly two recombination processes come into consideration. In a reaction of the type $\text{Rb} + \text{Rb} + \text{Rb}^+ \rightarrow \text{Rb}_2 + \text{Rb}^+$ the formation of a neutral molecule is catalyzed by the ion which carries away 2/3 of the energy released. If deeply bound Rb_2 molecules are produced binding energies of up to ~ 0.5 eV are released, in agreement with the measurement. A second possible recombination process, $\text{Rb} + \text{Rb} + \text{Rb}^+ \rightarrow \text{Rb}_2^+ + \text{Rb}$, produces a molecular ion and a neutral atom. However, as indicated in figure 3, the molecular ion, due to its higher mass, experiences a significantly shallower trap than the atomic ion and would immediately be lost for our parameter range. We thus infer that the ion at hand is Rb^+ . However, we cannot completely exclude the formation of an intermediate molecular ionic state which may subsequently dissociate.

In a third type of measurement we study the dependence of the three-body coefficient on the ion kinetic energy which we can tune by controlling the ion micromotion. For this we apply a static electric field ε perpendicular to the axis of the Paul trap and let the ion interact for $\tau = 8$ s with an atom cloud with $n_{\text{at}} \approx 1.0 \times 10^{12}$ cm⁻³. We find $P_{\text{threebody}}$ to increase roughly by a factor of 5 when reducing ε from 3.25 V/m to 0 V/m (Fig. 4a).

In order to express the electric field values in terms of kinetic energy we make use of the relation $E_{\text{eMM}} = c_{\text{trap}} \cdot \varepsilon^2 + E_{\text{res}}$ with c_{trap} a constant that depends on the trap configuration and the ion mass [15]. E_{res} stands for residual uncom-

pensated micromotion energy, e.g. due to rf phase delay between the trap electrodes. The ion energy can be expressed as $E_{\text{ion}} = c_{\text{dyn}} \cdot E_{\text{eMM}}$ [19]. c_{dyn} is a constant which depends on the atom-ion mass ratio and the spatial extension of the atom cloud and for our experiments can be estimated to be about 2 [17]. Since three-body coefficients often follow simple scaling laws, we attempt to describe our data with a power-law dependence of the form $K_3 \propto E_{\text{ion}}^\alpha$ within our simulation. We have taken care to also account for the energy dependence of the two-body interactions. Good agreement with the data is achieved for $\alpha = -0.43$, $E_{\text{res}} = 370 \mu\text{K} \cdot k_{\text{B}}$ and a maximal value for K_3 of 2.75×10^{-25} cm⁶/s (solid trace in Fig. 4b). For comparison, curves for exponents $\alpha = -0.5$ and $\alpha = -0.33$ (dashed and dotted traces, respectively) are shown as well. A residual energy $E_{\text{res}} = 370 \mu\text{K} \cdot k_{\text{B}}$ is a reasonable value for our current setup and in agreement with other measurements of ours [14].

In conclusion, we have studied three-body recombination involving a single trapped ion and two of its parent atoms at collision energies approaching the sub-mK regime. With a relatively simple model we can understand the two- and three-body collision dynamics and extract corresponding rate coefficients. We observe an increase of the three-body rate coefficient with decreasing collision energy, a behavior that can be expected to become crucial for future experiments targeting even lower temperatures. After a three-body event, ion energies on the order of 0.4 eV were measured, indicating that deeply bound molecules have been created. Since we have not observed Rb_2^+ ions, the formation of Rb_2 seems probable. The ion would then act as an atomic size catalyzer at mK temperature. It is an interesting question whether such catalyzing action could also be observable close to more massive objects such as carbon nanotubes [22]. Finally, as a byproduct of our investigations, we also observe sympathetic cooling of ions from energies in the 0.1 eV range back to mK temperatures.

The authors would like to thank Kilian Singer, Piet Schmidt, David Hume, Olivier Dulieu and Brett Esry for helpful discussions and information. This work was supported by the German Research Foundation DFG within the SFB/TRR21.

-
- [1] H. F. Hess, D. A. Bell, G. P. Kochanski, R. W. Cline, D. Kleppner, and T. J. Greytak, Phys. Rev. Lett., **51**, 483 (1983)
 - [2] B. D. Esry, C. H. Greene, and J. P. Burke, Phys. Rev. Lett., **83**, 1751 (1999)
 - [3] E. A. Burt, R. W. Ghrist, C. J. Myatt, M. J. Holland, E. A. Cornell, and C. E. Wieman, Phys. Rev. Lett., **79**, 337 (1997)
 - [4] F. Ferlaino and R. Grimm, Physics, **3**, 9 (2010)
 - [5] N. Spethmann, F. Kindermann, S. John, C. Weber, D. Meschede, and A. Widera, arXiv:1204.6051v1 (2012)
 - [6] R. Côté and A. Dalgarno, Phys. Rev. A, **62**, 012709 (2000)
 - [7] A. Grier, M. Cetina, F. Oručević, and V. Vuletić, Phys. Rev. Lett., **102**, 223201 (2009)
 - [8] C. Zipkes, S. Palzer, C. Sias, and M. Köhl, Nature, **464**, 388 (2010)

- [9] S. Schmid, A. Härter, and J. Hecker Denschlag, *Phys. Rev. Lett.*, **105**, 133202 (2010)
- [10] K. Ravi, S. Lee, A. Sharma, G. Werth, and S. A. Rangwala, arXiv:1112.5825v1 (2011)
- [11] F. H. J. Hall, M. Aymar, N. Bouloufa-Maafa, O. Dulieu, and S. Willitsch, *Phys. Rev. Lett.*, **107**, 243202 (2011)
- [12] W. G. Rellergert, S. T. Sullivan, S. Kotochigova, A. Petrov, K. Chen, S. J. Schowalter, and E. R. Hudson, *Phys. Rev. Lett.*, **107**, 243201 (2011)
- [13] S. Schmid, A. Härter, A. Frisch, S. Hoinka, and J. Hecker Denschlag, *Rev. Sci. Instrum.*, **83**, 053108 (2012)
- [14] To be published
- [15] D. J. Berkeland, J. D. Miller, J. C. Bergquist, W. M. Itano, and D. J. Wineland, *Journal of Applied Physics*, **83**, 5025 (1998)
- [16] R. G. DeVoe, *Phys. Rev. Lett.*, **102**, 063001 (2009)
- [17] C. Zipkes, L. Ratschbacher, C. Sias, and M. Köhl, *New J. Phys.*, **13**, 053020 (2011)
- [18] M. Cetina, A. Grier, and V. Vuletić, arXiv:1205.2806v1 (2012)
- [19] Due to the non-thermal energy distribution of the ion immersed in the atom cloud [16, 17] we use the median as an energy measure.
- [20] Performing numerical simulations we find that the ion is very unlikely to leave the atom cloud even at the high energy power-law tail of the energy distribution. More strikingly, we experimentally observe the signature of ion ejection only upon minimization of the ion micromotion, in stark contrast to the expectations of the quoted heating mechanism.
- [21] K. Singer, U. Poschinger, M. Murphy, P. Ivanov, F. Ziesel, T. Calarco, and F. Schmidt-Kaler, *Rev. Mod. Phys.*, **82**, 2609 (2010)
- [22] M. Gierling, P. Schneeweiss, G. Visanescu, P. Federsel, M. Häffner, D. Kern, T. Judd, A. Günther, and J. Fortágh, *Nat. Nano.*, **6**, 446 (2011)